

Origin of fluctuations in atmospheric pressure arc plasma devices

S. Ghorui and A. K. Das

Laser and Plasma Technology Division, Bhabha Atomic Research Centre, Trombay, Mumbai, India

(Received 27 March 2003; revised manuscript received 29 May 2003; published 26 February 2004)

Fluctuations in arc plasma devices are extremely important for any technological application in thermal plasma. The origin of such fluctuations remains unexplained. This paper presents a theory for observed fluctuations in atmospheric pressure arc plasma devices. A qualitative explanation for observed behavior on atmospheric pressure arc plasma fluctuations, reported in the literature, can be obtained from the theory. The potential of the theory is demonstrated through comparison of theoretical predictions with reported experimental observations.

DOI: 10.1103/PhysRevE.69.026408

PACS number(s): 52.75.Hn, 52.70.-m, 81.15.Rs

Thermal plasma technology has been established as a promising tool for state of the art industrial applications. The arc plasma device is the heart of related processes for generation of plasma. Depending on the regime of operation, an inherent fluctuation in plasma parameters is always associated with such devices. The growth of thermal plasma technologies is mainly hampered due to lack of control on these fluctuations [1]. A complete understanding of this phenomenon is long awaited and is believed to have a strong impact on the growth of thermal plasma technology [1]. However, no satisfactory theory is available that can predict the measurable fluctuations observed in such devices. Fluctuations observed experimentally in such devices are analyzed using tools of dynamical analysis and found to follow a gradual transition from the nonchaotic to chaotic regime [2–3] under variation in control parameters. The present paper attempts to introduce a theory of observed arc fluctuations in atmospheric pressure thermal plasma devices. The earlier concept that the observed fluctuations in arc plasma devices are random and beyond control needs drastic modification in light of the experimental evidence and subsequent analyses [2,3]. The present theoretical work together with earlier experimental works establishes arc plasma fluctuations as chaotic. Axiomatically, therefore, these fluctuations are controllable. Next, an attempt was made to validate the theoretical estimates against a wide range of experiments available in the literature. Application of the theory to reported experiments by the authors and by Brillhac *et al.* has been presented in order to demonstrate the potential of the present technique.

In any arc plasma device, an arc is established between anode and cathode through some flowing gas (plasmagen

gas). The arc heats the gas through ohmic heating and transforms it into weakly ionized plasma. This is then used for associated processing work. Arc starts from the cathode, proceeds through the current channel in the gas and finally joins the anode at some position as shown in Fig. 1(a). Associated electromagnetic forces, guides the current to enter anode normally at the arc root. On application of dc voltage and superimposition of a high frequency field, an arc is established between the cathode and the anode. The root or the point of connection of the arc on the electrode is governed by minimum energy consideration commensurate to the condition on the surface. In an arc plasma torch, the roles of cathode and anode are completely different. In the conventional torch, cathode is a water-cooled thoriated tungsten rod or a button with a tapered tip. The tip is thoriated to bring down the work function for efficient emission of electrons. Either through thermionic or field emission or both, electrons are emitted from this tip and passed through the gas constituting a current channel called an arc. The typical heat fluxes to the cathode remains at 1–2%, whereas the anode receives more than 10% of the total power. Moreover, the incoming cold plasma gas, introduced in a swirl near the cathode, cools it more effectively. It is true that the arc moves on the surface of the cathode due to the emission process, cathode jets, and electromagnetic forces. However, the cathode surface is much smaller in size and the effect on the voltage, optical, and acoustic emission is dominantly from the anode arc root dynamics. The present paper looks at the anode arc root. The intense external cooling provided creates a cold boundary next to the anode. As arc is established, the entire current passes through a small cylindrical zone (area $\sim \text{mm}^2$) which

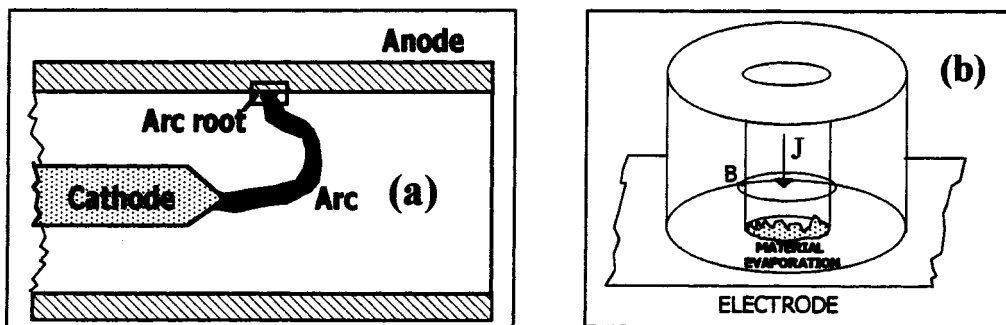


FIG. 1. (a) Formation of arc in an arc plasma torch. (b) Schematic of the model of near arc root region.

electrically connects the main arc to the electrode. Since the current densities are extremely high ($\sim \text{kA}/\text{cm}^2$), this region is heated with temperature of the order of thousands of K through intense ohmic heating. Considering the physical situation and the extremely low density of the hot plasma, assumption of cylindrical symmetry in near arc root region as shown in Fig. 1(b) is justifiable. The vertical dimension in the arc root region is defined by the typical radial dimensions of the arc column in a plasma torch (5–10 mm) and the extent of the thermal and electrical boundary layer at the electrode (~ 1 mm). The radial dimension is established from the experimental data through optical measurement of the arc attachment zone [4] which again are of the order of 1–2 mm. Gradient in temperature is determined by sublimation point (~ 2000 K) temperature of material of the electrode at the arc root and joule heating of the core of the plasma. The typical gradient would be $\sim 10^6$ K/m. At temperature $\sim 10^4$ K and pressure of near atmospheric, the near arc root plasma column remains at local thermal equilibrium (LTE) defined by a single temperature. The energy input to the anode spot is roughly balanced by evaporation and a nearly constant temperature is maintained on the surface [5]. The anode spot temperature is above boiling point for most materials and therefore, a high vapor pressure exists for the material evaporated [5]. The evaporated material strongly diffuses into the zone near arc root. Because of the tiny area of the spot, extremely high current density appears in the region. This in association with self-magnetic field produces a compressive force on the current carrying plasma column just above the anode spot. The compressive force results in increased current density that in turn generates more heat and tries to counteract the compressive force. All these together make the near arc root region a highly nonlinear system with complicated time dependence. The degree of complication depends on the arc current and existing temperature of the near arc root zone.

Analysis of dynamic behavior is carried out through modeling this region near the arc root. Underlying instability in the arc root region disturbs the balance of the forces under which the arc root stays at a particular position. Consequently, resulting force imbalance leads the arc root to shift from one equilibrium position to another. The arc root, wherever it shifts, assumes the cylindrical shape for the near electrode region with nearly equal size. Presented results are obtained for assumed radial dimension of 2 mm and vertical dimension of 1 mm of the near arc root instability zone.

To model the phenomenon we assume that the tiny cylindrical arc column near arc root having vertical dimension d and radius R possess uniform temperature in the radial direction and a vertical temperature gradient of ΔT . Over the steady field components, instability induces fluctuating temperature component T and metal concentration component S . We also assume that metal vapor enters the plasma with almost zero velocity so that the separate momentum conservation equation is not required. Under the Bousinesq approximation one assumes density constant in analyses except for thermal expansion cases. Such approximations are reasonably valid for near arc root region considered. For the tiny arc root region [Fig. 1(b)], conservation of mass, momentum,

heat, metal vapor concentration together with Maxwell's equations gives the following differential equations for evolution of the fluctuating quantities under such approximation.

(i) Conservation of heat

$$\frac{\partial T}{\partial t} - w \frac{\Delta T}{d} + \vec{v} \cdot \vec{\nabla} T = \kappa \nabla^2 T, \quad (1)$$

where $\kappa = k/\rho s$ is diffusivity of heat and $\vec{v} = u\hat{r} + v\hat{\theta} + w\hat{z}$ is velocity. k , ρ , and s are thermal conductivity, density, and specific heat, respectively.

(ii) Conservation of metal

$$\frac{\partial S}{\partial t} - w \frac{\Delta S}{d} + \vec{v} \cdot \vec{\nabla} S = \kappa_s \nabla^2 S. \quad (2)$$

Here S is metal concentration and κ_s is the diffusivity of material.

(iii) Conservation of momentum. Considering normal stress force due to pressure (p), tangential stress force due to viscosity (ν), gravitational force due to expansion of fluid and addition of material, and Lorentz force due to interaction of current density (J) with magnetic field (B), the momentum conservation equation can be written as

$$\frac{\partial \vec{v}}{\partial t} + \vec{v} \cdot \vec{\nabla} \vec{v} = -\frac{1}{\rho_0} \vec{\nabla} p + \nu \nabla^2 \vec{v} + \vec{g} \alpha T - \vec{g} \beta S + \frac{1}{\rho_0} \vec{J} \times \vec{B}. \quad (3)$$

Here we have used the equation of state for the fluctuation of density (ρ) in which α and β are defined as $\Delta \rho = \rho_0(-\alpha T + \beta S)$.

(iv) Conservation of mass. Using Bousinesq approximation

$$\vec{\nabla} \cdot \vec{v} = 0. \quad (4)$$

(v) Maxwell's equation

$$\vec{J} = \frac{1}{\mu_0} (\vec{\nabla} \times \vec{B}), \quad \vec{J} = \sigma_C (\vec{E} + \vec{v} \times \vec{B}),$$

$$\vec{\nabla} \times \vec{E} = -\frac{\partial \vec{B}}{\partial t}, \quad \vec{\nabla} \cdot \vec{B} = 0. \quad (5)$$

σ_C and μ_0 are the electrical conductivity and permittivity, respectively. Considering cylindrical symmetry of B produced due to J , Eq. (5) gives

$$\frac{\partial \vec{B}}{\partial t} + \vec{v} \cdot \vec{\nabla} \vec{B} = \eta_B \nabla^2 \vec{B} + (\vec{B} \cdot \vec{\nabla}) \vec{v}$$

where

$$\eta_B = 1/\mu_0 \sigma_C. \quad (6)$$

Approximating $\vec{B} = B_\theta(r) \hat{\theta}$ and $\vec{J} = J_0 \hat{z}$ for the tiny column near the arc root

$$\frac{\partial B}{\partial t} = \phi(B, v) - \mu_0 J_0 u + \eta_B \nabla^2 B$$

where

$$\phi(B, v) = (\vec{B} \cdot \vec{\nabla})v + u \frac{B}{r}. \quad (7)$$

Introducing stream function ψ such that $u = dr/dt = \partial\psi/\partial z$, $w = dz/dt = -\partial\psi/\partial r$, $\Gamma(\psi, \phi) = -\vec{V} \cdot \vec{\nabla} \phi$, $\eta = \partial u/\partial z - \partial w/\partial r = \nabla^2 \psi$, removing the pressure term, taking the curl, and after nondimensionalization the set of governing equations reduces to

$$\frac{\partial \eta}{\partial t} = \Gamma(\psi, \eta) + \sigma \nabla^2 \eta - R_l \sigma \partial_r T + R_s \sigma \tau \partial_r S - \frac{2}{R} \sigma \xi Q \partial_z B, \quad (8)$$

$$\frac{\partial T}{\partial t} = \Gamma(\psi, T) - \partial_r \psi + \nabla^2 T, \quad (9)$$

$$\frac{\partial S}{\partial t} = \Gamma(\psi, S) - \partial_r \psi + \tau \nabla^2 S, \quad (10)$$

$$\frac{\partial B}{\partial t} = \phi(v, B) - 2dR^{-1} \partial_z \psi + \xi \nabla^2 B, \quad (11)$$

where all the parameters are dimensionless and R_l , R_s , σ , ξ , τ , and Q are Rayleigh number, solute Rayleigh number, Prandtl number, magnetic Prandtl number, ratio of solute to thermal diffusivities, and Chandrasekhar number, respectively, defined as

$$R_l = \frac{g \alpha \Delta T d^3}{\kappa \nu}, \quad R_s = \frac{g \alpha \Delta S d^3}{\kappa \nu}, \quad \sigma = \frac{\nu}{k},$$

$$\xi = \frac{\eta_B}{k}, \quad \tau = \kappa_S / \kappa, \quad Q = \frac{B_0^2 d^2}{\mu \rho_0 \eta_B \nu}.$$

Equations (8)–(11) are now expressible in the form

$$\partial_t L Y = M_\lambda Y + N(Y), \quad (12)$$

where Y is plasma field vector, L is a nonsingular linear operator, M is a linear operator, and N is a strictly nonlinear operator:

$$Y = \begin{bmatrix} \psi \\ T \\ S \\ B \end{bmatrix}, \quad L = \begin{bmatrix} \nabla^2 & 0 & 0 & 0 \\ 0 & 1 & 0 & 0 \\ 0 & 0 & 1 & 0 \\ 0 & 0 & 0 & 1 \end{bmatrix},$$

$$M = \begin{bmatrix} \sigma \nabla^4 & -R_l \sigma \partial_r & R_s \sigma \tau \partial_r & -2R^{-1} \sigma \xi Q \partial_z B \\ \partial_r & \nabla^2 & 0 & 0 \\ \partial_r & 0 & \tau \nabla^2 & 0 \\ -2dR^{-1} \partial_z & 0 & 0 & \xi \nabla^2 \end{bmatrix}. \quad (13)$$

We now employ the technique devised by Arneodo, Coulet, and Spiegel [6] (ACS) for derivation of amplitude equation. Under suitable boundary conditions [6], the linear version of Eq. (12) admits a solution of the form

$$Y = Y_{mn}^* \Lambda_{mn} e^{st}, \quad (14)$$

where Y_{mn} is a constant four-component vector and

$$\Lambda_{mn} = \begin{bmatrix} \sin(mar) \sin(n\pi z) \\ \cos(mar) \sin(n\pi z) \\ \cos(mar) \sin(n\pi z) \\ \sin(mar) \cos(n\pi z) \end{bmatrix}.$$

Here m and n are integers specifying the mode of instability. The operation E^*F leads to a new vector G such that the components of G are products of respective components of E and F . Upon substitution, Eq. (12) gives

$$M_{mn}(\lambda) = \begin{bmatrix} \sigma q_{mn}^4 & ma \sigma R_l & -ma \sigma \tau R_s & 2n \pi \xi \sigma Q R^{-1} \\ -ma & -q_{mn}^2 & 0 & 0 \\ -ma & 0 & -\tau q_{mn}^2 & 0 \\ -2n \pi d R^{-1} & 0 & 0 & -\xi q_{mn}^2 \end{bmatrix}, \quad L_{mn}(a) = \begin{bmatrix} -q_{mn}^2 & 0 & 0 & 0 \\ 0 & 1 & 0 & 0 \\ 0 & 0 & 1 & 0 \\ 0 & 0 & 0 & 1 \end{bmatrix}$$

with $q_{mn}^2 = m^2 a^2 + n^2 \pi^2$. A characteristic equation corresponding to the linear part of the eigenvalue Eq. (12) gives the value of s in the solution Y . For lowest order instability ($m=1, n=1$) we have

$$s^4 + \Pi_3 s^3 + \Pi_2 s^2 + \Pi_1 s + \Pi_0 = 0,$$

$$\Pi_0 = q^2(q^6 - a^2 R_l + a^2 R_s - 4d \pi^2 R^{-2} Q) \sigma \tau \xi,$$

$$\Pi_1 = -a^2 \sigma (\tau + \xi) R_l + a^2 \sigma \tau (1 + \xi) R_s - 4d \pi^2 R^{-2} \sigma \xi (1 + \tau) Q + (\sigma \tau + \sigma \xi + \tau \xi + \sigma \tau \xi) q^6,$$

$$\Pi_2 = -a^2 \sigma q^{-2} R_l + a^2 \sigma \tau q^{-2} R_s - 4d \pi^2 R^{-2} \sigma \xi q^{-2} Q + (\sigma + \tau + \xi + \sigma \tau + \sigma \xi + \tau \xi) q^4,$$

$$\Pi_3 = q^2(1 + \tau + \sigma + \xi). \quad (15)$$

For just the onset of instability $s = i\omega$ and $\omega \rightarrow 0$. The condition where all the three roots of Eq. (18) vanishes needs to satisfy the condition: $\Pi_0 = \Pi_1 = \Pi_2 = 0$ [6] and the values of the controlling parameters in such situation (critical condition) come to be

$$R_{lo} = \frac{q^6(\sigma + \tau + \xi)}{a^2\sigma(\tau - 1)(\xi - 1)}, \quad R_{so} = \frac{q^6\tau^2(1 + \sigma + \xi)}{a\sigma(\tau - 1)(\xi - \tau)},$$

$$Q_0 = \frac{q^6(1 + \sigma + \tau)\xi^2}{c_m\sigma(\xi - 1)(\xi - \tau)}. \quad (16)$$

where $c_m = 4d\pi^2R^{-2}$. For these values of parameters, M_{mn} vanishes and Y spans in null space with basis vectors (ϕ, ψ, χ) . Near the onset of instability Y can be split into two parts one in stable space $\Xi(x, y, z)$ and the other in null space spanned by basis vectors (ϕ, ψ, χ) and Y can be written as [6]

$$Y = [A(t)\phi + B(t)\psi + C(t)\chi] * \Lambda_{11}(x, z) + \Xi(x, z, t). \quad (17)$$

Substituting Eq. (17) into Eq. (12) the amplitude equation for the linearized system comes to be

$$\ddot{A} + C_2\dot{A} + C_1A + C_0A = 0, \quad (18)$$

where

$$C_0 = \frac{\Pi_0}{\Pi_3}, \quad C_1 = \frac{\Pi_1}{\Pi_3} - \frac{\Pi_0}{\Pi_3^2} \quad \text{and} \quad C_2 = \frac{\Pi_2}{\Pi_3} - \frac{\Pi_1}{\Pi_3^2} + \frac{\Pi_0}{\Pi_3^3}.$$

A nonlinear extension of Eq. (18) can be written as

$$\ddot{A} + C_2\dot{A} + C_1A + C_0A = \zeta(A), \quad (19)$$

where ζ is the nonlinear contribution. Noting that Eqs. (8)–(11) remain invariant under operation ψ to $-\psi$, T to $-T$, S to $-S$, B to $-B$, Eq. (19) is required to satisfy $\zeta(-A) = -\zeta(A)$. This shows the system to be free from second order nonlinearity and the lowest order nonlinearity will be $O(A^3)$. Over a wide range of studies such as stratified shear flow with unsteady critical layer [7], instability of geophysical flows [8], stability of compressible flows [9], it has been observed that cubic nonlinearity dominates the evolution of instability wave amplitude. Therefore, we expect Eq. (19), containing third order nonlinearity, will be good enough to predict the system behavior. Correctness of the assumption in this particular case will be justified if outcome of theory matches well with experimental observation. Therefore, an approximate form of the nonlinear amplitude equation for the system can be written as

$$\ddot{A} + C_2\dot{A} + C_1A + C_0A = C_4A^3. \quad (20)$$

In Eq. (20), C_4 has no effect other than scaling the amplitude [6]. Therefore, for study of system behavior, only two values of C_4 are sufficient: $+1$ and -1 . Using the new time scale $s = C_2t$ and scale factor for amplitude as $A = C_2^{3/2}F$, Eq. (20) reduces to

$$\ddot{F} + \Omega_2\dot{F} + \Omega_1F + \Omega_0F = \pm F^3, \quad (21)$$

where

$$\Omega_0 = C_0/C_2^2, \quad \Omega_1 = C_1/C_2^3, \quad \Omega_2 = 1, \quad (22)$$

and all derivatives are with respect to the new time scale. For a given plasma operating condition, coefficients in the nonlinear amplitude equation ultimately depend on arc current and various thermophysical properties of the plasma such as density, electrical conductivity, thermal conductivity, viscosity, specific heat, diffusivity, etc. An explicit form of such dependence comes out from expressions of the coefficients given in Eqs. (15) and (18). Once the temperature of the instability zone and gas forming the plasma are identified, all mentioned thermophysical properties of the generated plasma are known from the property table of respective plasma gases available in literature [10] and coefficients can be computed. As all the coefficients (C_0, C_1, C_2) are known for a given plasma operating condition, Eq. (21) can be solved to get time dependence of amplitude of plasma field vector Y . The underlying instability will be reflected in all measurable signals emitted from the plasma subjected to associated other conditions. Details on measurement scheme, device details, accuracy, and specifications of measurement devices are available in Refs. [1] and [2]. The electronic component of the weakly ionized plasma will instantaneously respond to the generated fluctuation in electric field and transfer a part of their energy to the neutrals through elastic collisions. The energy transfer, modulated according to fluctuation, induces pressure perturbation and generates an acoustic wave of speed c in the plasma [10]. Depending on dimension (l) of the plasma, this acoustic signal can be detected mostly undistorted but enveloped by a response function $f(\omega) = \omega^{-1} \sin(\omega l/2c)$ [11]. The amplitude of the acoustic signal is proportional to the derivative of total power input to the plasma [2,3,10]. In our experiment (comprised of more than 250 runs under various conditions) it has been found that generated acoustic signal is directly proportional to $A(t)$. Once unenveloped acoustic signal [$A(t)$] is obtained, the fluctuating behavior of power [$\Theta(t)$] inside the plasma is obtained just by integrating $A(t)$. Under constant current operation, $\Theta(t)$ will be proportional to the arc voltage [$V(t)$]. However, the response of the device to $V(t)$ will be distorted due to the fact that the device responds to power fluctuation by shifting position of arc root so that minimum energy configuration is maintained. Shifting of the arc root depends on the surface morphology of electrodes and balance of number of forces [12]. Ideally the total optical output from the plasma should follow the fluctuation in power. The sound wave generated inside the plasma creates regions of contraction and rarefaction. The resulting density perturbation creates perturbation in index of refraction, which also fluctuates according to the underlying dynamics. As a result, the optical signal transmitted through the medium will be modulated by the sound wave and scattering and refraction will occur. Among all the signals, the theoretical fluctuation will be best reflected in acoustic signal due to extreme sensitivity. A detectable acoustic wave can be excited with as

little as 1 mW power fluctuation [13]. The highest distortion will be observed for total optical output. However, upon analysis all of them will reflect the signature of same underlying phenomenon. Experiment on actual system supports each of these facts [2,3].

The present system transits from steady behavior to regular oscillatory and finally to chaotic state as the value of control parameter changes. Upon gradual variation of control parameter values, system is found to follow period doubling route to chaos. It is observed that in the prechaotic state the system indeed remains very sensitive to the chosen value of control parameter. However, once the system enters into chaotic regime, system behavior becomes relatively insensitive to the chosen value of control parameters. Under typical operating conditions, the regime of coefficients automatically lead atmospheric pressure arc plasma system to run in fully chaotic region. This is the best region to compare outcome of the theory with experiment. At this stage, shape of the attractor, its dimension, value of Lyapunov exponent and main characteristic frequencies in the continuous power spectrum, estimated in the paper, are very close to those obtained experimentally. This gives a range in the value of theoretical inputs corresponding to realized experimental conditions. All values near about the realized one result in nearly identical outcome. This fact is confirmed both theoretically and experimentally. For very large values of control parameters, systems exhibit catastrophic behavior in terms of sudden extinction of the arc as observed in experiments.

Most of the arc plasma devices are operated using constant current power supply units. Therefore, arc current is measured externally through a potential divider unit with an accuracy $\sim 98\%$. It has been observed that all nearby currents (up to $\pm 2-3\%$), result in similar behavior both experimentally and theoretically, once the system operates in chaotic mode. Current influences the behavior through both ohmic heating as well as electromagnetic forces. However, the system is fairly insensitive to the practically realizable temperature gradient of the region. In the theory, temperature gradient appears in all gravity related terms. Insensitiveness to gravity related terms indicate that the discussed phenomenon of fluctuation will be observed irrespective of orientation of the device. This is an experimentally true fact.

The theory can predict exact oscillatory behavior once arc current and temperature of the instability originating zone is specified. However, for validation accurate assignment of values are essential. In practice, the arc root forms inside the hollow anode, it is hidden behind the electrode and surrounded by highly luminous plasma. Over and above this, it changes its position very fast. Due to such complications, it is extremely difficult to measure correct temperature of the near arc root instability zone experimentally. In view of these difficulties, an indirect innovative approach has been adopted in the paper. We compute the fluctuations, analyze their dynamics properties at various temperatures, and compare with experimentally observed data for the best match. The validation is more focused on justification of the physical situation and trend of behavior at varying physical conditions. As observed in Fig. 2, the near criticality region is achieved near 5900 K for $I=400$ A, for argon plasma. The observed match

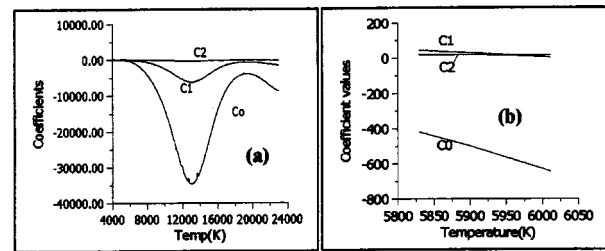


FIG. 2. Variation of coefficients with temperature for argon plasma. (a) An overall view. (b) Near criticality.

between experiment and theory for this temperature under the realized coefficient values is displayed in Fig. 3. They are in fairly good agreement with corresponding experiments reported in Refs. [2], [3]. Extensive steady state numerical simulations and experiments available in literature suggest that existence of such temperature at the near arc root region is indeed appropriate for $I=400$ A. Similar is true for the presented comparison in Fig. 4 with experiment by Brillhac *et al.* also.

Regarding observed typical fluctuations in arc plasma devices, the primary question to researchers arises whether they are random or follow some specific rule. Whether it is possible to generate similar fluctuations from the underlying governing equations of the system or not. Since the system is dynamic, it is not possible to obtain an exact one to one correspondence between experimental and theoretical time series. Moreover, while coming out from the system, generated signals are distorted by many other factors as discussed. However, they must carry similar features. For example, time dependent governing equations of the system should generate fluctuations having at least similar characteristic frequencies and the time series should show a similar trend in time behavior.

Figure 3(a) presents comparison of time series. As mentioned, a one to one correspondence is not observed between them. However, their time evolutions exhibit identical trends. This is more explicit in a comparison of their power spectra [Fig. 3(e)]. Both the spectra show continuous nature and presence of identical characteristic frequencies. It is observed that in the high frequency domain, frequencies observed in the theoretical spectra are absent in the experimental one. This could be the result of presence of the envelop function in frequency domain which has the effect of diminishing high frequency components in power spectra as discussed. Similar agreements are observed in the results presented in Fig. 4.

The behavior of the system is determined through the value of the coefficients. Since the fluctuation phenomenon is assumed to be arising out of marginal stability C_1 and C_2 vary slowly with temperature, whereas C_0 varies significantly (Fig. 2). Thermophysical property data, particularly the transport properties such as thermal conductivity, viscosity, and diffusivities are prone to error due to lack of accurate data on collision properties that may have inaccuracy as large as 15%. In the present case, for a particular system, inaccuracy in thermophysical property data has the only effect of shifting position of occurrence of marginal stability in

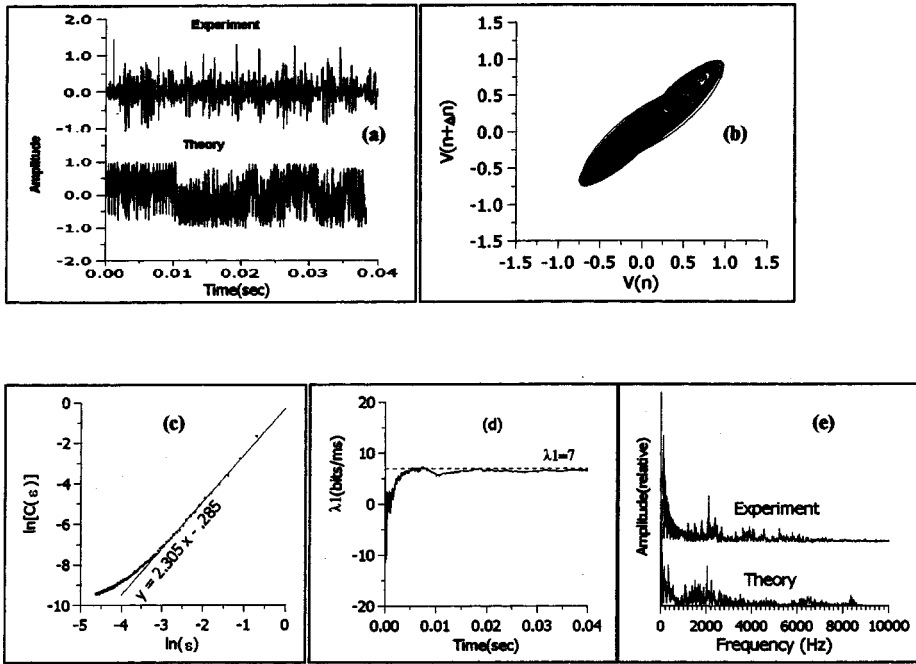


FIG. 3. Results from theory. (a) Time series. (b) Attractor. (c) Dimension computation. (d) Largest Lyapunov exponent computation. (e) Power spectra [$\Omega_0 = -143, I = 400$ A].

temperature space. Therefore, occurrence of a particular trend of behavior is brought out more clearly than exact point of occurrence in temperature space.

The results presented in this paper are computed for most common plasma forming gas argon. However, nitrogen, air and mixture of gases such as a small volume of hydrogen in argon are also used in some cases as plasma gas. Coefficients have been calculated for such gases and it has been observed that similar near criticality behavior are obtainable for them also. However, for nitrogen such behavior is obtained at relatively higher temperatures compared to that in argon. In practice, such an increase in temperature is always observed experimentally when one changes gas from argon to nitrogen in a plasma device. For argon plasma, variation of the coefficients (C_i) with temperature are shown in Fig. 2 for arc current 400 A. Similar coefficient regions appear at relatively higher plasma temperature for lower arc currents. Variation of C_i with T becomes sharper for higher currents. It is seen that the possible values of coefficients near criticality ($C_i = 0$) are $C_0 - ve$, $C_1 + ve$, and $C_2 + ve$. Under such a condition, Eq. (21) gives fluctuating time series only for $-\Omega_0 > \Omega_1/2$ and steady solution for $-\Omega_0 < \Omega_1/2$. There is a range of possible parameter values for which a variety of oscillatory behaviors are possible. For a given operating con-

dition, the tiny plasma column near arc root will stay at a particular average temperature. It is expected that for higher arc currents, accepted coefficient values by the system will shift towards possible values at relatively higher temperatures. We find $C_0 \approx -450$, $C_1 \approx 100$, $C_2 \approx 1.5$ is a set of possible coefficient values near which the system can operate. This gives $\Omega_0 \approx -130$, $\Omega_1 \approx 50$, $\Omega_2 \approx 1$. At all currents near this region, C_1 and C_2 remain nearly constant but $-C_0$ increases significantly for small increment in temperature. Therefore, the effect of increase in current can be studied just by increasing $-\Omega_0$ keeping Ω_1 and Ω_2 fixed. For the experimental system [2–3], fluctuations observed at currents 100, 200, 300, and 400 A, are obtained for Ω_0 values -139.295 , -140 , -142.5 , and -143 , respectively, with $\Omega_1 = 50$, and $\Omega_2 = 1$. Figures 3(a)–3(e) show, respectively, comparison of time series, attractor, computation of dimension, comparison of evolution of largest Lyapunov exponent and comparison of power spectra for the time series obtained from theory for $\Omega_0 = -143$ (current=400 A). A good match is observed with experiments reported in Refs. [2] and [3]. Dimension is computed using an algorithm, verified rigorously through application in standard attractors having known dimension. The algorithm undoubtedly computes dimension correctly up to first decimal point. Lyapunov exponent is computed using a widely used algorithm developed by Alan Wolf [14]. In the algorithm as time increases, more and more numbers of sampled data points join the computation and computed exponent value tries to reach the actual one.

The theory has been applied to a number of important investigations, reported in contemporary literature [15–19]. Brillhac *et al.* have studied dynamic and static behavior of dc vortex plasma torches, having button type cathodes [15]. Fluctuation in arc voltage, arc current, electrical power, optical radiation, and acoustic signal generated from such de-

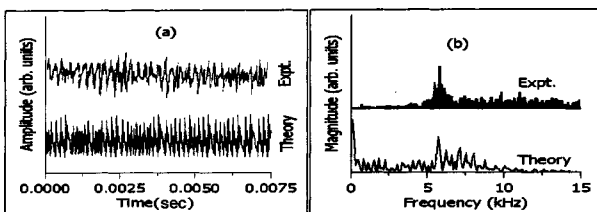


FIG. 4. Comparison with experiments by Brillhac *et al.* (a) Acoustic fluctuation. (b) Power spectra of acoustic signal [$I = 105$ A, $V = 379$ V, Flow=253 slpm].

vices are investigated in terms of time series, various dimensionless numbers, and frequency spectra of respective signals. They have performed similar study for dc vortex plasma torches having well type cathodes also [16]. Fluctuations in arc voltages under various arc currents are reported by Verdelle *et al.* for spray plasma torches [17]. Fluctuating behavior of the Sulzer Metco F4 dc plasma gun has been investigated by Dorier *et al.* [18]. Temporal, spectral, and statistical analyses are carried out on fluctuating arc voltage and optical output from the torch. Various features of arc root fluctuation such as voltage jump and spot lifetime are studied in detail for upstream and down stream striking of dc spray plasma torch by Codert *et al.* [19] and specific trends are observed. The theory has been applied to all of them and it has been observed that the theory successfully generates all reported features of underlying instability studied in these experiments. Typical agreement between experiment and theory in such study looks as presented in Fig. 4.

At present it is clearly established that the fluctuations in atmospheric pressure arc plasma devices severely affect their performance related to plasma processing applications [1]. It reduces the electrode life by more than 100 h and reduces process efficiency by more than 10%. As the arc burns, jumps, and zigzags over the electrodes without any control, the electrode life, repeatability, and process efficiency are severely affected. A methodology is therefore sought for on-line monitoring and control of such device/processes. Earlier [2,3], the authors had established experimentally the existence of chaotic behavior in arc plasma devices. The most important impact of the current work is in providing a systematic theoretical basis for these experimental observations from the basic governing principles.

Unlike random systems, chaotic systems are controllable. Chaotic systems consist of infinite number of unstable periodic orbits. Any one or some of these unstable periodic orbits can be stabilized and the choice can be made to achieve best system performance of the device. A large variety of dynamics is obtainable from the system. One can think of various

modes of perturbation to tailor the same device for various purposes. In this context, stabilization of high period orbit will be particularly advantageous for arc plasma systems. In such a case most regions of the attractor is visited and the system actually passes through different states but remains controlled and not in chaotic mode.

An Ott-Grebogi-Yorke method for controlling chaos in dynamical system, which has been applied to large number of systems, has the potential to be implemented in the present case. Although, the exact technical protocol is not yet finalized, a possible technique could be providing a pressure or a voltage perturbation to the system to change phase space dynamics and stabilize specific orbits. Presently, work is being undertaken in our laboratory to implement such techniques. Once an arc plasma device achieves control over these fluctuations, it will be an extremely useful and reliable economic device for quality plasma processing work with high degree of reproducibility. One can think of excellent applications in the fascinating field of nanotubes and nanoparticles using plasma technology, where such fluctuations may vastly vary the growth of various nanoprocesses. Similar links in terms of technological implications can be established to electrode losses due to erosion, puncturing of device, sudden extinction of arc, change of surface conditions of the electrodes, change in operating characteristics of torch, etc. The present work is an attempt to provide a methodology to control all these nonlinear interactions occurring in arc plasma devices employing knowledge of nonlinear dynamics.

In conclusion we have reported a theory for observed fluctuations in atmospheric pressure arc plasma devices, explained the origin and behavior of emanated signals from such systems, and demonstrated the potential of the theory through computation of invariants of dynamics such as attractor, fractal dimension, largest Lyapunov exponent and power spectra.

The author would like to thank Dr. N. Venkatramani and Dr. A.K. Ray for their kind permission to carry out this work.

-
- [1] E. Pfender, *Plasma Chem. Plasma Process.* **19**, 1 (1999).
 [2] S. Ghorui, S.N. Sahasrabudhe, P.S.S. Murthy, A.K. Das, and N. Venkatramani, *IEEE Trans. Plasma Sci.* **28**, 253 (2000).
 [3] S. Ghorui, S.N. Sahasrabudhe, P.S.S. Murthy, A.K. Das, and N. Venkatramani, *IEEE Trans. Plasma Sci.* **28**, 2179 (2000).
 [4] R. Beudet and M.G. Drouet, *IEEE Trans. Power Appl.* **PAS-93**, 1054 (1974).
 [5] J.D. Cobine and E.E. Burger, *J. Appl. Phys.* **26**, 895 (1955).
 [6] A. Arneodo, P.H. Coulet, and E.A. Spiegel, *Geophys. Astrophys. Fluid Dyn.* **31**, 1 (1985).
 [7] M.E. Goldstein and S.W. Choi, *J. Fluid Mech.* **207**, 97 (1989).
 [8] G.R. Flierl, *J. Fluid Mech.* **197**, 349 (1998).
 [9] S.J. Lib, *J. Fluid Mech.* **224**, 551 (1991).
 [10] M. Boulos, P. Fuchais, and E. Pfender, *Thermal Plasmas, Fundamentals and Applications* (Plenum, New York, 1994), Vol. 1.
 [11] M. Fitaire and T.D. Monte, *Phys. Fluids* **15**, 464 (1972).
 [12] M.P. Collares and E. Pfender, *IEEE Trans. Plasma Sci.* **25**, 864 (1997).
 [13] M. Fitaire and T. Mantei, *Phys. Lett.* **29A**, 84 (1969).
 [14] A. Wolf, J.B. Swift, H.L. Swinney, and J.A. Vastano, *Physica D* **16**, 285 (1985).
 [15] J.F. Brilhac, B. Pateyron, G. Delluc, J.F. Coudert, and P. Fauchais, *Plasma Chem. Plasma Process.* **15**, 231 (1995).
 [16] F. Brilhac, B. Pateyron, J.F. Coudert, P. Fauchais, and A. Bouvier, *Plasma Chem. Plasma Process.* **15**, 257 (1995).
 [17] A. Verdelle, P. Fuchais, B. Dussoubs, and N.J. Themelis, *Plasma Chem. Plasma Process.* **18**, 551 (1995).
 [18] J. L. Dorier, Ch. Hollenstein, A. Salito, M. Loch, and G. Barbezat (unpublished).
 [19] F. Coudert, M.P. Planche, and P. Fauchais, *Plasma Chem. Plasma Process.* **16**, 211s (1996).